Oscillatory Combustion of Monopropellant Droplets

S. P. Chanin* and G. M. Faeth†
Pennsylvania State University, University Park, Pa.

A theoretical study of combustion response to imposed pressure oscillations was conducted for monopropellant droplets and sprays. A first-order perturbation analysis was used, yielding the linear response. Transient gas-phase phenomena were considered in some cases, but the bulk of the calculations assume a quasisteady gas phase. The calculations employed properties representative of hydrazine decomposition. Calculated steady combustion results and response predictions for large hydrazine droplets agreed favorably with earlier measurements. Droplet and spray response factors in excess of unity were found. High response was associated with high pressures (1000-10,000 kN/m^2), large droplets, large mean liquid temperature gradients, and frequencies near the characteristic frequency of the liquid-phase thermal wave. Spray response factors are lower than the response factor of the largest injected drop; however, a small percentage of large drops can still provide substantial response for the combustion process.

Nomenclature

A = constant, Eq. (9)
a = vapor pressure parameter
B = pre-exponential parameter
C_f, C_p = specific heat of liquid and gas
E = activation energy
f = spray size distribution function
K_1 = constant, Eq. (38)
L = heat of vaporization
L_f = vapor pressure parameter
M = molecular weight
m = mass flow rate per unit solid angle
N_0 = drop injection rate
n = reaction order
Pr, Pr_t = drop and spray response factors
p = pressure
Q = injected drop-size distribution
q = heat of combustion
R_s = radius ratio, Eq. (45)
R = gas constant
r = radial distance
T = temperature
t = time
v = radial velocity
w = reaction rate
Y = mass fraction
α = thermal diffusivity
β = specific-heat ratio, Eq. (1)
γ = specific-heat ratio
δ = reaction parameter
δ_f = constant, Eq. (1)
ϵ = amplitude of pressure oscillation
θ = Shvab-Zeldovitch variable, Eq. (17)
λ = thermal conductivity
ν_i', ν_i'' = stoichiometry parameters
ρ = density
ω = frequency

Subscripts

f = liquid
F = fuel
i = droplet center
L = large drop limit
S = small drop limit
s = surface
0 = steady-state quantity
1 = first-order quantity
∞ = far from droplet

Superscripts

0 = initial condition
$*$ = dimensional quantity

Presented as Paper 76-615 at the AIAA/SAE 12th Propulsion Conference, Palo Alto, Calif., July 26-29, 1976; submitted Aug. 3, 1976; revision received Nov. 29, 1976.

Index categories: Combustion Stability, Ignition, and Detonation; Combustion in Heterogeneous Media.

*Graduate Assistant, Department of Mechanical Engineering.
†Professor of Mechanical Engineering. Member AIAA.

Introduction

THERE have been several studies concerned with the open-loop combustion response of liquid-fuel droplets and surfaces, surrounded by diffusion flames.[1-5] The present investigation considers this problem for monopropellant droplets and sprays, where each droplet is surrounded by a premixed flame. In contrast to the diffusion flame process of bipropellants, where the combustion response is low, the present study has found that monopropellant droplets and sprays exhibit substantial response factors for droplet sizes and disturbance frequencies representative of high-frequency combustion instability in rocket engines.

The type of response under consideration does not involve the low-frequency regime where both liquid- and gas-phase processes are quasisteady, but rather conditions where transient liquid- and gas-phase phenomena, or thermal waves, are interacting with the combustion process. An earlier study considered this problem for a liquid monopropellant strand, where the simple geometry allowed direct response measurements.[6] A strand combustion model was found to provide a good description of both steady state and response characteristics. Encouraged by this result, the present investigation extends the model to the more practical case of monopropellant droplet and spray combustion.

The analysis involves a numerically integrated, first-order perturbation solution, with transient effects and property variations treated in the same manner as Ref. 6. Physical and chemical properties for the calculations were chosen to simulate hydrazine decomposition. In this case, the theory can be checked against the results of Ref. 6, as well as with reported experimental droplet burning rates under conditions representative of combustion chambers.[7]

Droplet Combustion Model

The model considers gas- and liquid-phase transient effects, and variable physical properties are treated in the gas phase. To simplify the analysis, forced convection was neglected, providing a spherically symmetric combustion process around

each drop. This limitation is less serious for monopropellants than bipropellants, since the response is greatest for monopropellants when the combustion zone is located near the liquid surface, a condition where combustion is not strongly affected by forced convection.[8,9] Combustion far from the droplet approximates evaporation without combustion; under these circumstances the response due to velocity effects has been found to be small.[1] Other evidence also suggests that regions of low droplet velocity are critical for combustion instability.[5]

The physical property assumptions in the gas phase are typical of other combustion response studies.[1-3,6] Molecular weights and specific heats of all species are equal and constant, the gas is ideal, the Lewis number is unity, $\rho\lambda$ is a constant, and radiation is neglected. Reaction is limited to the gas phase where it is assumed to be premixed, laminar, and following one-step, irreversible kinetics. Time lags associated with the reaction itself are neglected, i.e., the chemical reaction is locally quasisteady for local, instantaneous concentrations and temperatures in the region of reaction. Liquid-phase physical properties are assumed to be constant.

Similar to earlier response studies,[1,6] the ambient pressure is assumed to be oscillating with a long wavelength in comparison to the dimensions of the drop combustion field. The period of oscillation, however, is taken to be short in comparison to the total drop lifetime, and variations in the mean liquid-surface position during an oscillation are not considered. This assumption implies a low-frequency bound for a given drop size, below which the present analysis is no longer valid; specific frequencies for this limit are described later. Conditions near the thermodynamic critical point of the drop are not considered, and the instantaneous velocity of the liquid surface is neglected in comparison to radial gas velocities.

A common assumption for drop combustion studies is that the drop is heated uniformly to its wet-bulb temperature. It is generally recognized, however, that temperature gradients persist within drops throughout their lifetime, as artifacts of the heat-up period. The high mean combustion rate of monopropellants increases the possibility of liquid temperature gradients.[10] In order to study the implications of mean liquid temperature gradients on monopropellant combustion response, two limiting cases were treated, a) mean liquid temperature varying as though a quasisteady combustion wave was propagating toward the unheated center of the drop, and b) mean liquid temperature constant at the wet-bulb temperature.

The coordinate system is fixed with respect to the mean position of the liquid surface. In this coordinate system an observer perceives that the mass flux of fuel in the liquid phase is time varying, and the process appears similar to porous sphere combustion. For N chemical species in the system, the decomposition reaction is defined as follows:

$$\sum_{i=i}^{N} \nu_i' [i] \rightarrow \sum_{i=i} \nu_i'' [i]$$

In order to simplify the notation, variables are made dimensionless as follows:

$$a=a^*/p_0^* \qquad t=t^*\lambda_{\infty_0}^*/\rho_{\infty_0}^* C_p^* r_s^{*2}$$

$$E=E^*/R^*T_{\infty_0}^* \qquad T=T^*/T_{\infty_0}^*$$

$$L=L^*/C_p^*T_{\infty_0}^* \qquad v=v^*\rho_{\infty_0}^* C_p^* r_s^*/\lambda_{\infty_0}^*$$

$$L_f=L_f^*/R^*T_{\infty_0}^* \qquad \beta=C_f^*/C_p^*$$

$$\dot{m}=\dot{m}^* C_p^* r_s^* \lambda_{\infty_0}^* \qquad \delta_f=\alpha_f^*/\alpha_{\infty_0}^*$$

$$p=p^*/p_0^* \qquad \lambda=\lambda^*/\lambda_{\infty_0}^*$$

$$q=q^*/C_p^*T_{\infty_0}^* \qquad \rho=\rho^*/\rho_{\infty_0}^*$$

$$r=r^*/r_s^* \tag{1}$$

The equations of conservation of mass and energy in the liquid, $r<1$, are

$$\rho_f r^2 v_f = \dot{m}_f \tag{2}$$

$$\frac{\partial T}{\partial t} + v_f \frac{\partial T}{\partial r} = \frac{\delta_f}{r^2}\frac{\partial}{\partial r}\left(r^2 \frac{\partial T}{\partial r}\right) \tag{3}$$

The equations of conservation of mass, and species and energy in the gas, $r>1$, are

$$\frac{\partial \rho}{\partial t} + \frac{1}{r^2}\frac{\partial}{\partial r}(\rho r^2 v) = 0 \tag{4}$$

$$\dot{m} = \rho r^2 v \tag{5}$$

$$\rho\frac{\partial Y_i}{\partial t} + v\frac{\partial Y_i}{\partial r} = \frac{1}{r^2}\frac{\partial}{\partial r}\left(r^2\lambda\frac{\partial Y_i}{\partial r}\right) + \nu_i w \quad i=1,N \tag{6}$$

$$\rho\frac{\partial T}{\partial t} + v\frac{\partial T}{\partial r} = \frac{1}{r^2}\frac{\partial}{\partial r}\left(r^2\lambda\frac{\partial T}{\partial r}\right) + \left(\frac{\gamma-1}{\gamma}\right)\frac{dp}{dt} + q\,w \tag{7}$$

where

$$w = A\,p^n T^{\delta-n} Y_F{}^n \exp(-E/T) \tag{8}$$

and A is a reaction parameter related to the drop size

$$A = \frac{C_p^* B^* r_s^{*2} T_{\infty_0}^{*\delta}}{\lambda_{\infty_0}^*}\left(\frac{P_0^*}{M^* R^* T_{\infty_0}^*}\right)^n \tag{9}$$

The assumed form for gas property variations implies

$$\rho T = \rho\lambda = p \tag{10}$$

Since the liquid is incompressible, the boundary condition at the center of the drop is

$$T = T_i \tag{11}$$

The two cases noted earlier involve T_i equal to the injection temperature and the wet-bulb temperature, respectively.

In addition to continuity of temperature and pressure at the liquid surface, $r=1$, four other conditions must be satisfied at this point. Conservation of mass requires

$$\dot{m} = \dot{m}_f \tag{12}$$

Conservation of energy yields

$$\lambda_f\frac{\partial T}{\partial r}\Big)_{s-} = \lambda\frac{\partial T}{\partial r}\Big)_{s+} - \rho v[(1-\beta)T + L] \tag{13}$$

The insolubility of the liquid phase to non-fuel gases provides

$$\lambda\frac{\partial Y_F}{\partial r}\Big)_{s+} = \rho v(Y_F - 1) \tag{14}$$

Finally, the fuel mass fraction is related to the surface temperature and pressure through the Clausius-Clapeyron equation

$$Y_F = a\exp(-L_f/t) \tag{15}$$

Far from the liquid surface, $r=\infty$, all the fuel is consumed, and the temperature is only a function of time,

$$Y_F=0 \qquad T=T(t) \tag{16}$$

where $T(t)$ is a known function depending upon the specified pressure variation.

Equations (6)-(16) can be simplified by introducing a Shvab-Zeldovitch variable, θ, based on the fuel mass fraction and the temperature.

$$\theta=q\ Y_F+T \tag{17}$$

A perturbation analysis was used to solve this set of equations, by decomposing the pressure variation into a constant mean pressure and an oscillatory component having a small amplitude, ϵ. Noting that pressure is only a function of time and seeking oscillatory solutions implies

$$\begin{aligned} p(t)&=1+\epsilon\ e^{i\omega t}\\ T(r,t)&=T_0(r)+\epsilon T_1(r)e^{i\omega t}\\ \theta(r,t)&=\theta_0(r)+\epsilon\ \theta_1(r)e^{i\omega t}\\ \dot m(r,t)&=\dot m_0(r)+\epsilon\ \dot m_1(r)e^{i\omega t}\\ \dot m_f(t)&=\dot m_{f0}+\epsilon\ \dot m_{f1}e^{i\omega t} \end{aligned} \tag{18}$$

where T_1, θ_1, $\dot m_1$, and $\dot m_{f1}$ are complex quantities. The quantities T_0, θ_0, etc., represent steady combustion of the drop; while T_1, θ_1, etc., provide the first-order oscillatory component which yields the linear response of the combustion process.

Substituting Eqs. (17) and (18) into Eqs. (2)-(16) yields the following zero-order, steady-state equations

$$\dot m_{f0}=\dot m_0=\text{const} \tag{19}$$

$$r\le 1 \qquad \frac{\mathrm{d}}{\mathrm{d}r}\left(r^2\frac{\mathrm{d}T_0}{\mathrm{d}r}-\frac{\dot m_0}{\rho_f\delta_f}T_0\right)=0 \tag{20}$$

$$r>1 \qquad \frac{\mathrm{d}}{\mathrm{d}r}\left(r^2T_0\frac{\mathrm{d}\theta_0}{\mathrm{d}r}-\dot m_0\theta_0\right)=0 \tag{21}$$

$$\frac{\mathrm{d}}{\mathrm{d}r}\left(r^2T_0\frac{\mathrm{d}T_0}{\mathrm{d}r}-\dot m_0T_0\right)+r^2q\ w_0=0 \tag{22}$$

where

$$w_0=A\overset{n}{q}T_0^{\delta-n}(\theta_0-T_0)^n\exp(-E/T_0) \tag{23}$$

The boundary conditions on these equations are

$$r=1 \qquad r=0 \qquad T=T_i \tag{24}$$

$$1+\lambda_f\frac{\mathrm{d}T_0}{\mathrm{d}r}\Big)_{s-}=T_0\frac{\mathrm{d}T_0}{\mathrm{d}r}\Big)_{s+}-\dot m_0[(1-\beta)T_0+L] \tag{25}$$

$$T_0\frac{\mathrm{d}(\theta_0-T_0)}{\mathrm{d}r}\Big)_{s+}=\dot m_0(\theta_0-T_0-q) \tag{26}$$

$$\theta_0-T_0=a\ q\ \exp(-L_f/T_0) \tag{27}$$

$$r=\infty \qquad \theta_0=T_0=1 \tag{28}$$

The zero-order equations are sufficiently general to allow either adiabatic or nonadiabatic ambient conditions. Since most combustion chambers are nearly adiabatic, and monopropellants do not involve a local enthalpy defect in any stream, adiabatic combustion was assumed, to simplify the calculations. This assumption is only strictly true when there are temperature gradients in the liquid phase, since bulk heating causes small enthalpy defects within the spray. Adiabatic combustion provides the following zero-order compatability condition

$$q=1-\beta\ T_i+L \tag{29}$$

Introducing T_{0s} as the liquid surface temperature, Eq. (20) can be integrated to give the liquid-phase temperature distribution

$$\frac{T_0-T_i}{T_{0s}-T_i}=\exp\left[\frac{\dot m_0}{\rho_f\delta_f}\left(1-\frac{1}{r}\right)\right] \tag{30}$$

Upon application of the outer boundary conditions for adiabatic combustion, integration of Eq. (21) yields $\theta_0=1$. The zero-order problem then involves the solution of a single, nonlinear, second-order differential equation, Eq. (22). Equations (25-28) provide four boundary conditions, the two required for a second-order differential equation and two that determine T_{0s} and $\dot m_0$.

Equation (22) was integrated using a fourth-order Hamming predictor-corrector algorithm. Following Ref. 6, the boundary condition at $r=\infty$ was handled by an asymptotic expansion of Eq. (22) at large r. A shooting technique was employed, integrating toward the liquid surface, and iterating using the Newton-Raphson method until all surface boundary conditions were satisfied. The details of the calculation procedure are presented in Ref. 11.

Incorporating the zero-order results, the first-order perturbation equations are as follows

$$r\le 1 \qquad \dot m_{f1}=\text{const} \tag{31}$$

$$\frac{\mathrm{d}}{\mathrm{d}r}\left(r^2\frac{\mathrm{d}T_1}{\mathrm{d}r}\right)-\frac{\dot m_0}{\rho_f\delta_f}\frac{\mathrm{d}T_1}{\mathrm{d}r}-\frac{i\omega r^2}{\delta_f}T_1=\frac{\dot m_{f1}}{\rho_f\delta_f}\frac{\mathrm{d}T_0}{\mathrm{d}r} \tag{32}$$

$$r>1 \qquad T_0{}^2\frac{\mathrm{d}\dot m_1}{\mathrm{d}r}-i\omega r^2T_1=-i\omega r^2T_0 \tag{33}$$

$$\frac{\mathrm{d}}{\mathrm{d}r}\left(r^2T_0\frac{\mathrm{d}\theta_1}{\mathrm{d}r}\right)-\dot m_0\frac{\mathrm{d}\theta_1}{\mathrm{d}r}-\frac{r^2i\omega\theta_1}{T_0}=-r^2\left(\frac{\gamma-1}{\gamma}\right)i\omega \tag{34}$$

$$\begin{aligned} &\frac{\mathrm{d}}{\mathrm{d}r}\left(r^2T_0\frac{\mathrm{d}T_1}{\mathrm{d}r}\right)-\dot m_0\frac{\mathrm{d}T_1}{\mathrm{d}r}+\frac{\mathrm{d}}{\mathrm{d}r}\left(r^2T_1\frac{\mathrm{d}T_0}{\mathrm{d}r}\right)\\ &+r^2qw_0\left[(\delta-n)\frac{T_1}{T_0}+n\left(\frac{\theta_1-T_1}{\theta_0-T_0}\right)+\frac{ET_1}{T_0^2}\right]\\ &-\left[\frac{r^2i\omega T_1}{T_0}\right]=\dot m_1\frac{\mathrm{d}T_0}{\mathrm{d}r}-r^2\left(\frac{\gamma-1}{\gamma}\right)i\omega-r^2q\ w_0n \end{aligned} \tag{35}$$

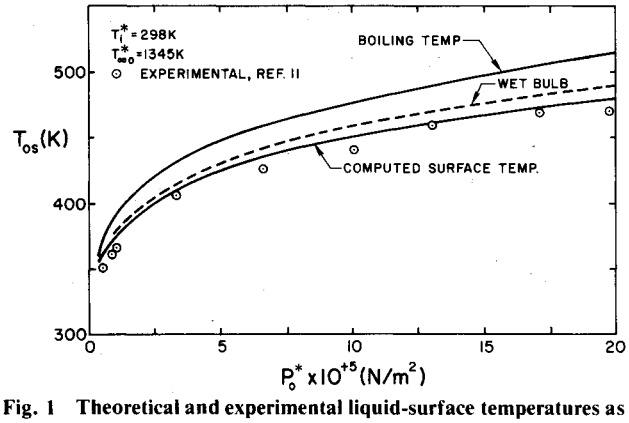

Fig. 1 Theoretical and experimental liquid-surface temperatures as a function of pressure.

The boundary conditions on these equations are

$$r=0 \qquad T_1=0 \tag{36}$$

$$r=1 \qquad \dot{m}_{f1}=\dot{m}_1 \qquad T_{1s}=T_{1s+}$$

$$\lambda_f \frac{dT_1}{dr}\Big)_{s-} = T_1 \frac{dT_0}{dr}\Big)_{s+} + T_0 \frac{dT_1}{dr}\Big)_{s+} - \dot{m}_1[(1-\beta)T_0+L]$$

$$-\dot{m}_0(1-\beta)T_1$$

$$T_0 \frac{d(\theta_1-T_1)}{dr}\Big)_{s+} - T_1 \frac{dT_0}{dr}\Big)_{s+} = \dot{m}_0(\theta_1-T_1)$$

$$+ \dot{m}_1(1-T_0-q)$$

$$\theta_1 - T_1 = a\, q \exp(-L_f/T_0)\left(\frac{L_f T_1}{T_0^2}-1\right) \tag{37}$$

Far from the droplet, θ_1 and T_1 must approach a constant value.

$$r=\infty \qquad \theta_1=T_1=K_1 \tag{38}$$

The value of K_1 depends upon the case under consideration. For an unsteady gas phase, since $\theta_1=\theta_1(t)$ at large r, the constant can be determined by considering the behavior of Eq. (35) at large r. In this case, $K_1=(\gamma-1)/\gamma$, which is the form for isentropic flow.

In the case of a quasisteady gas phase, with transient effects still important in the liquid phase, K_1 is the amplitude of the ambient temperature variation due to the varying energy content of the liquid at the surface of the droplet (resulting from transient energy storage in the liquid phase). In this case, K_1 becomes a second eigenvalue in the solution to be determined along with $\dot{m}_1$. When the liquid phase also becomes quasisteady, the value of K_1 approaches zero, since in the absence of transient storage in the liquid phase, Eq. (29) must be satisfied for adiabatic combustion.

The equations for the first-order problem are linear, requiring a total of seven boundary conditions for the completely unsteady case. Equations (36-38) provide eight boundary conditions, allowing determination of the eigenvalue $\dot{m}_{f1}$. The linearity of the equations was exploited to eliminate iteration to satisfy the boundary conditions; asymptotic expansions were used to handle boundary conditions at large and small r; and numerical integration was employed to solve the equations. The details of the calculation procedure may be found in Ref. 11.

The physical property values used in the calculations are given in Ref. 6. The chemical-kinetic parameters are summarized in Table 1. These values were found to give a good representation of both the steady and oscillatory combustion characteristics of hydrazine strands at pressures greater than 100 kN/m^2, where hydrazine exhibits second-order decompositions kinetics.[6]

Steady Droplet Combustion

To check the accuracy of the zero-order model, predicted and measured liquid temperatures and burning rates were compared. Under the unity Lewis number assumption, the liquid surface temperature is independent of geometry, and comparison can be made with the strand combustion experiments of Ref. 6. The results are illustrated in Fig. 1 as a function of pressure. The data correspond to adiabatic combustion with $T_i=298$ K. The agreement between theory and experiment is within experimental accuracy throughout the pressure range of the measurements.

Table 1 Kinetic properties of the calculations

B^*(m^3/kg-s)	8.385×10^{10}
E^*(kJ/kg-mol)	111,700
n	2
δ	0

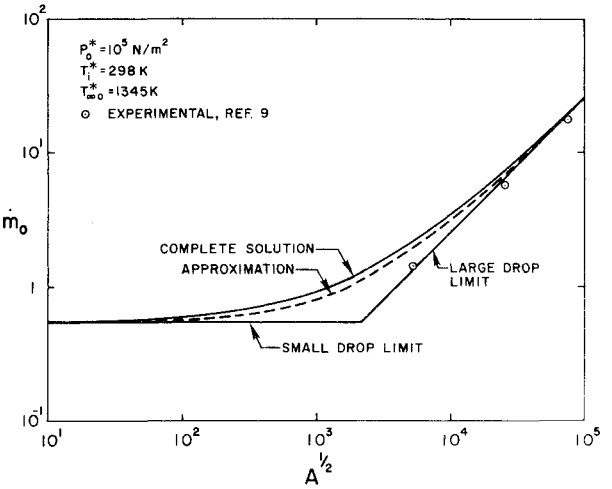

Fig. 2 Theoretical and experimental steady drop gasification rates for non-wet-bulb conditions.

Liquid temperatures for the wet-bulb case, where the droplet temperature is uniform, are also plotted in Fig. 1. For the wet-bulb case, liquid surface temperatures are higher since no energy is required to raise the fuel to the vaporization temperature.

Figure 2 shows the steady burning rate as a function of $A^{1/2}$, which is proportional to drop diameter, at a pressure of 100 kN/m^2. The burning rate approaches two limits; one for small droplets which is independent of A, and one for large droplets where the burning rate is proportional to $A^{1/2}$.

The small drop limit represents conditions where vaporization occurs without appreciable reaction. At this limit

$$\dot{m}_{0S}=1-T_{0s}+(q-1)\ln(1-(1-T_{0s})/q) \tag{39}$$

where T_{0s} can be determined from Eq. (27), noting $\theta_0=1$. Equation (39) corresponds to the well-known droplet evaporation rate expressions, for the present variable property gas-phase model.

The large drop limit represents conditions where the combustion zone is very close to the liquid surface and spherical curvature effects are negligible. This situation is equivalent to strand combustion and a single burning rate eigenvalue

$$A_s = \frac{B^* T_{\infty 0}{}^{*\delta} \lambda_{\infty 0}{}^*}{(\rho_{\infty 0}{}^* v_{\infty 0}{}^*)^2 C_p{}^*}\left(\frac{P_0{}^*}{M^* R^* T_{\infty 0}{}^*}\right)^n \tag{40}$$

represents the combustion rate per unit area for a given T_i and pressure. At the large drop limit, the burning rate is given by

$$\dot{m}_{0L}=(A/A_s)^{1/2} \tag{41}$$

An approximate formula for the mass burning rate over the entire range of A can be obtained by simply adding the small and large droplet components at each value of A

$$\dot{m}_0 \doteq \dot{m}_{0S}+\dot{m}_{0L} \tag{42}$$

This approximation is illustrated in Fig. 2, and was found to yield a maximum error of 12% over the range of the present calculations.

Data on hydrazine drop combustion have been reported by Allison and Faeth.[7] Various drop sizes were burned in a

Table 2 Summary of steady combustion calculations

p_0^* (kN/m^2)	T_{0s}^*(K)	T_0^* (K)	$\dot{m}_{0S}$	A_s
Non-wet-bulb combustion, $T_i^* = 298$ K				
100	374	1345	0.544	1.432×10^7
1000	450	1345	0.509	1.432×10^7
10,000	562	1345	0.454	1.432×10^7
Wet-bulb combustion				
100	376	1417	0.603	6.205×10^6
1000	457	1498	0.629	2.660×10^6
10,000	582	1623	0.668	8.162×10^5

Table 3 Drop lifetimes (msec)

	Initial drop diam (μm)			
p_0^*(kN/m^2)	20	80	140	200
Non-wet-bulb combustion, $T_i^* = 298$ K				
100	1.58	23.4	66.9	128
1000	1.35	13.4	30.2	48.9
10,000	0.507	2.69	5.00	7.34
Wet-bulb combustion				
100	1.41	20.5	57.7	109
1000	0.955	8.15	17.3	27.2
10,000	0.179	.842	1.52	2.00

combustion gas under decomposition conditions at ambient temperatures in the range 1660-2530 K. To test the present results, these measurements were extrapolated to a 1345 K ambient temperature representative of adiabatic combustion with $T_i = 298$ K. The results are shown on Fig. 2; the data falls near the large drop limit and is in fair agreement with the predictions.

Burning rates for wet-bulb conditions are similar to Fig. 2, with a slight increase in burning rate for all values of A. Results at other pressures are also qualitatively similar. The transition between the small and large drop limits falls approximately in the range $10^4 < A < 10^9$; which corresponds to droplet diameters of 25-7500 μm at atmospheric pressure, with both limits proportional to p^{-1}. Thus the size range of most sprays falls largely in the transition region. At high pressures, however, a greater percentage of the drops in sprays fall in the large drop regime.

Some of the important results of the calculations are summarized in Table 2. While A_s is relatively independent of pressure at non-wet-bulb conditions, A_s decreases with increasing pressure for the wet-bulb case, increasing the burning rate. This is due to the higher flame temperatures for wet-bulb combustion at high pressures. The small droplet burning rate varies largely due to the changes in the temperature difference between the ambient gas and the drop surface as the pressure changes.

Equation (42) can be employed to obtain a simple expression for the mean drop size variation as a function of time. Overall conservation of drop mass requires

$$\frac{dr_s^*}{dt^*} = \frac{-\dot{m}_0^*}{\rho_f^* r_s^{*2}} \tag{43}$$

Integrating Eq. (43) and placing the result in dimensionless form yields the following implicit equation for the variation of radius with time

$$t\dot{m}_{0L/\rho f} = 1 - R_s + (\dot{m}_{0S}/\dot{m}_{0L})\ln[(\dot{m}_{0S} + \dot{m}_{0L}R_s)/(\dot{m}_{0S} + \dot{m}_{0L})] \tag{44}$$

where

$$R_s = r_s/r_s^0 \tag{45}$$

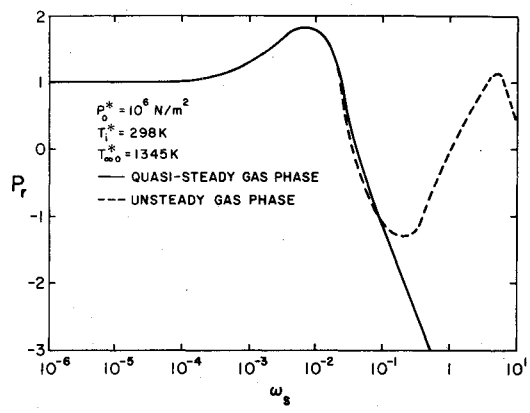

Fig. 3 Large droplet response as a function of frequency for non-wet-bulb combustion.

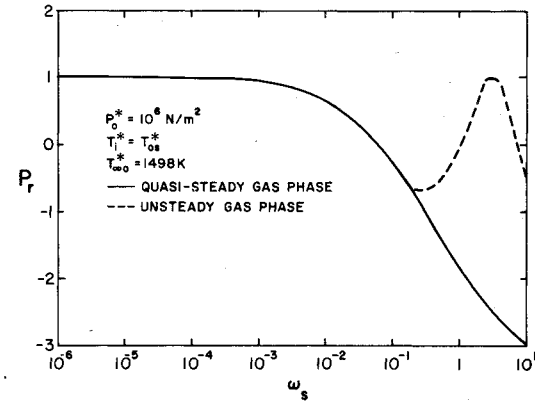

Fig. 4 Large droplet response as a function of frequency for wet-bulb combustion.

In Eq. (44), t and $\dot{m}_{0L}$ are both based on the initial drop radius. Setting $R_s = 0$ in Eq. (44) yields the lifetime of a drop. Typical lifetimes for hyrazine combustion at various pressures are summarized in Table 3.

The response portion of the present analysis is not valid at periods of oscillation comparable to the lifetime of a drop. Since drop lifetime decreases with size, this provides a minimum size that can be considered by the analysis for given conditions. High-frequency combustion instability is usually associated with the frequency range 500-30,000 Hz,[5] having oscillation periods of 0.03-2 msec. For given frequency, pressure, etc., this minimum size can be estimated from Table 3.

Droplet Combustion Response

The droplet burning rate response function[5]

$$P_r = Re\{\dot{m}_1/\dot{m}_0\} \tag{46}$$

is utilized to represent response. This function specifies that portion of the burning rate oscillation which is in-phase with the pressure oscillation. A necessary condition for instability is that some drops have response values on the order of unity (the exact value depends on the damping present) at a point in the chamber where the pressure is varying. Sufficient conditions for instability depend on the summed response of all drops within the chamber, which is considered when spray response is treated.

The greatest response was encountered at the large drop limit; Fig. 3 and 4 illustrate typical results for these conditions for both wet- and non-wet-bulb combustion. The dimensionless frequency corresponds to strand combustion,[6] and is defined as follows

$$\omega_s = (A_s/A)\omega \tag{47}$$

Table 4 Positive response regions for large hydrazine drops

p_0*(kN/m^2)	Liquid transient range (Hz)	Gas transient range (Hz)	Min. r_s large drop limit (μm)[b]
Non-wet-bulb combustion, $T_i = 298$ K			
100	<1.8	270-1,900	7500
1000	<84	2,100-170,000	750
10,000	<1,800	27,000	75
Wet-bulb combustion			
100	<2.0	330-1,500	7500
1000	<130	2,100-18,000	750
10,000	<6,700[a]	6,700[a]-190,000	75

[a]Liquid transient ans gas transient ranges separated at the minimum point in the response curve where $Pr = 0.14$.
[b]Corresponds to $A = 10^9$.

Results for both the transient and quasisteady gas-phase models are illustrated.

At low frequencies, where both phases are quasisteady, the response approaches unity. This follows because the burning rate is proportional to pressure for steady strand combustion under a second-order reaction.[6] For non-wet-bulb conditions, as the frequency increases, a response peak is observed at frequencies near the characteristic frequency of the liquid-phase thermal wave. This peak is absent for the wet-bulb case. Examining results over the entire range of the calculations, indicates that the peak is only present when there is a gradient in the mean liquid temperature at the liquid surface. The magnitude of the peak increases as the liquid temperature gradient increases and is highest for non-wet-bulb combustion at high pressures, where the higher liquid surface temperature for a given value of T_i, and faster mean burning rate, results in the steepest liquid temperature gradient. Thus, while liquid temperature gradients may not have a large effect on monopropellant drop lifetime predictions,[10] it appears that the presence of such gradients is an important factor for combustion response.

At frequencies on the order of $\omega_s = 10^{-1}$, the analysis allowing for transient gas-phase effects diverges from the quasisteady gas-phase analysis, and yields a second response peak that is associated with the gas-phase thermal wave. The response reaches unity in this region, and the peak is present for both wet- and non-wet-bulb conditions.

Table 4 summarizes the frequency regimes where large drops have positive response as a function of pressure. The drop size corresponding to the onset of the large drop limit, $A = 10^9$ is also listed. At pressures below 1000 kN/m^2, positive response due to gas-phase transient effects falls in the frequency range associated with acoustic instability, 500-30,000 Hz, but the drop sizes for the large drop limit are too large for typical sprays. At pressures above 1000 kN/m^2, liquid-phase transient response is more significant. The large drop regime also represents more realistic drop sizes in this range. Due to the high frequency of gas-phase transient phenomena, further calculations for drop sizes in the transition region were limited to the assumption of a quasisteady gas phase.

Figure 5 illustrates response in the transition region as a function of frequency for non-wet-bulb combustion. The response generally increases as A, or the drop size, increases. Results for the large drop limit are also shown on the figure, behavior in the transition region approaches the large drop limit for A in the range 10^9-10^{10}. The peak in the response curve only occurs for non-wet-bulb combustion at higher values of A. Thus, both strong premixed combustion effects and liquid-phase temperature gradients are necessary for a response peak to develop near the characteristic frequency of the liquid-phase thermal wave. Droplets evaporating with little reaction near the surface generally exhibit low or negative response throughout the frequency range, in

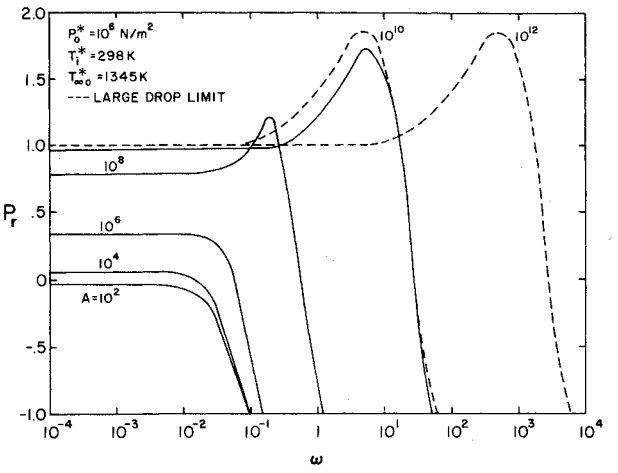

Fig. 5 Droplet response as a function of frequency and size for non-wet-bulb combustion.

agreement with earlier results for bipropellant drop combustion where fuel evaporation, without premixed combustion, also dominates the process.[1] The results shown in Fig. 5 are typical of other pressure conditions; additional plots may be found in Ref. 11.

Spray Combustion Model

For a given pressure field, a combustion chamber becomes unstable when the total response of all the drops exceeds the available damping. Since the droplet response calculations indicated that only certain drop sizes exhibit significant positive response, at a given frequency, it was of interest to determine whether entire sprays provided sufficient response for combustion instability. In order to simplify the work, the spray model assumes that the pressure field is identical for all parts of the spray, and complete combustion of the drops is accomplished within the combustion chamber. As before, forced convection effects are neglected. Under these circumstances, the spatial distribution of the spray droplets is immaterial, and the spray is described by the distribution function $f^*(r_s^*)$, which gives the total number of drops in the spray per unit radius range about r_s^*.

Under the present assumptions, the total spray response may be defined similar to the response of a single drop

$$Pr_t = Re\left(\int_0^\infty \dot{m}_l^* f^* \mathrm{d}r_s^* \Big/ \int_0^\infty \dot{m}_0^* f^* \mathrm{d}r_s^*\right) \tag{48}$$

representing the portion of the burning rate perturbation of the entire spray that is in-phase with the pressure oscillation. The droplet burning rate response function (46) can be introduced in Eq. (48) to yield

$$Pr_t = \int_0^\infty \dot{m}_0^* Pr f^* \mathrm{d}r_s^* \Big/ \int_0^\infty \dot{m}_0^* f^* \mathrm{d}r_s^* \tag{49}$$

The single drop analysis provides Pr and $\dot{m}_0^*$ as a function of drop size; therefore, Eq. (49) can be evaluated once the spray distribution function is known.

For steady mean conditions, noting that f^* represents the entire spray, the spray equation presented by Williams[12] becomes

$$\frac{\mathrm{d}}{\mathrm{d}r_s^*}\left(f^* \frac{\mathrm{d}r_s^*}{\mathrm{d}t^*}\right) = Q^* \tag{50}$$

where $Q^*(r_s^*)$ describes the rate of droplet production by the injector per unit radius range about r_s^* (production by collisions should be included as well, but this component was not considered here).

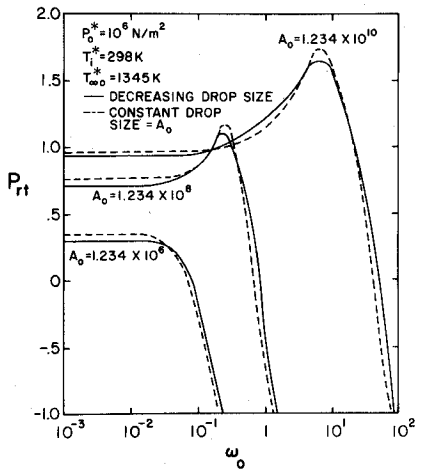

Fig. 6 Monodisperse spray response as a function of frequency and initial drop size for non-wet-bulb combustion.

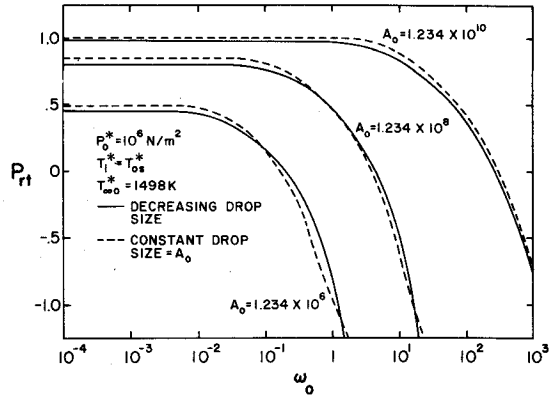

Fig. 7 Monodisperse spray response as a function of frequency and initial drop size for wet-bulb combustion.

Polydisperse sprays must be considered on a case-by-case basis. For a monodisperse spray, where all drops are formed at a fixed size r_s^{*0}, the results are particularly simple. In this case, integration of Eq. (50) and simplification using Eq. (43) yields

$$f^* = \rho_f r_s^{*2} N_0 / m_0^* \qquad r_s^* < r_s^{*0} \tag{51}$$

During the present calculations, m_0^* was evaluated using the approximate form given by Eq. (42). Since Pr is not available in analytic form, the response was evaluated by numerical integration, even for monodisperse sprays. The details of the calculations for both monodisperse and polydisperse sprays are given in Ref. 11.

Spray Combustion Response

Figure 6 illustrates the response of a monodisperse spray at a pressure of 1000 kN/m^2 for non-wet-bulb combustion. The dimensionless frequency ω_0 and the reaction rate parameter A_0 are based on the initial drop radius. The solid lines represent the entire spray, whereas the dashed lines correspond to the assumption that all drops in the spray have constant size given by A_0. The response peaks for the two cases occur at approximately the same frequency, with the magnitude of the spray response peak slightly overestimated when the drop size is taken to be constant. The reduction in the spray response is due to the reduced response of the smaller drops in the spray. Figure 7 presents similar results for wet-bulb combustion; there is little difference in general behavior, except for the absence of response peaks in this case.

Results for several polydisperse spray distributions are illustrated in Fig. 8 for non-wet-bulb injection at a pressure of 1000 kN/m^2. Three different sized droplets are injected, with distributions ranging from 100% large droplets to 100% small drops. The total response approaches unity when the two largest sized drops comprise only about 11% of the injected mass, corresponding to about 0.3% of the droplet injection rate; suggesting that even a very small percentage of large drops in the spray can result in substantial positive response. This behavior follows, since large drops form an appreciable fraction of the population of a spray due to their long lifetime, in comparison to small drops, which disappear almost immediately. For example, when the two largest sized drops comprise only 11% of the injected spray mass, droplets originating from these groups provide 90% of the mass of fuel in the burning spray. The findings were similar at other

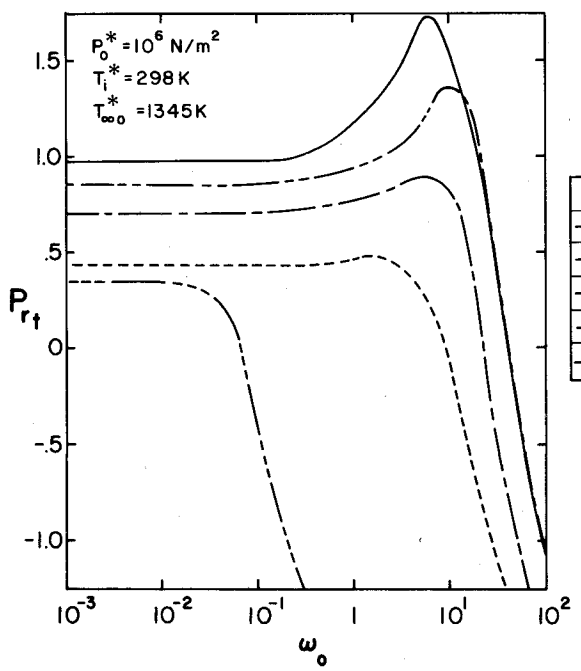

	% MASS IN CHAMBER			% DROPS/SEC. INJECTED			% MASS/SEC. INJECTED		
A_o(X10^8)	123	10	.0123	123	10	.0123	123	10	.0123
———	100[a]	0	0	100[a]	0	0	100[a]	0	0
- - - - -	10	30	60	.001	.053	99.946	.1	1.4	98.5
—·—·—	60	30	10	.005	.315	99.68	3.4	7.7	88.9
———	49.5	49.5	1.0	.05	4.98	94.97	11.47	51.78	36.75
———	0	0	100[a]	0	0	100[a]	0	0	100[a]

[a]ALL DROPS IN THE SPRAY ARE AT A CONSTANT SIZE A_o

Fig. 8 Polydisperse spray response as a function of frequency.

pressures for both wet- and non-wet-bulb combustion, except response peaks greater than unity are not observed for wet-bulb combustion.

Summary and Conclusions

An earlier theoretical model, which gave good predictions of monopropellant strand combustion response,[6] was extended to consider monopropellant droplets and sprays. Linear response was examined, employing first-order perturbation analysis. Calculations were conducted using the properties of hydrazine decomposition, due to the availability of data to test some aspects of the model for this material. The investigation was limited to the interaction of the combustion process with thermal waves in the liquid and gas, as opposed to the response associated with the entire droplet lifetime. The very high-frequency regime where inertial effects are important was not considered.

The conclusions of the study are as follows:

1) In some cases, the response of monopropellant drops and sprays approaches and exceeds unity for drop sizes and frequencies representative of high-frequency combustion instability, providing a viable mechanism for this phenomena. This is in contrast to the diffusion flame process of bipropellant combustion that yields relatively low response values.[5]

2) Response due to liquid-phase interactions is greatest for large drops, having mean liquid-phase temperature gradients at high pressures. Response factors in excess of unity were limited to conditions where a liquid-phase temperature gradient is present and the response increases as the gradient increases. Therefore, whereas internal temperature gradients due to drop heat-up have only a minor influence on lifetime characteristics,[10] this phenomena appears to be very important for instability behavior.

3) Large drops have a second response peak of order unity at frequencies associated with gas-phase transient effects. Except at low pressures, the frequency range of this peak is higher than the range generally associated with high-frequency combustion instability. The behavior of this peak for drops having sizes in the transition region was not examined and deserves further attention. The present results suggest that while the gas phase can be considered to be quasisteady for lifetime calculations at low pressures, important contributions to the response can be overlooked by neglecting transient gas-phase effects.

4) For the quasisteady gas-phase assumption, the response of a monodisperse spray is less than the response of the initial sized drop, due to the reduced response of small drops, although the frequency range of the response peak is similar.

5) Response depends strongly on the initial spray size distribution for a polydisperse spray; however, even a small percentage of large drops can provide appreciable response due to their long lifetimes and large response.

Acknowledgment

This work was supported by NASA Grant NGR 39-009-077, under the technical management of R. J. Priem of the Lewis Research Center.

References

[1]Tien, J. S. and Sirignano, W. A., "Unsteady Thermal Response of the Condensed-Phase Fuel Adjacent to a Reacting Gaseous Boundary Layer," *Proceedings of the Thirteenth Symposium (International) on Combustion*, The Combustion Institute, Pittsburgh, 1971, pp. 529-539.

[2]Strahle, W. C., "Periodic Solutions to a Convective Droplet Burning Problem: The Stagnation Point," *Proceedings of the Tenth Symposium (International) on Combustion*, The Combustion Institute, Pittsburgh, 1965, pp. 1315-1325.

[3]Strahle, W. C., "Unsteady Reacting Boundary Layer on a Vaporizing Flat Plate," *AIAA Journal*, Vol. 3, June, 1965, pp. 1195-1198.

[4]Williams, F. A., "Response of a Burning Fuel Plate to Sound Vibrations," *AIAA Journal*, Vol. 3, Nov. 1965, pp. 2112-2124.

[5]Harrje, D. T., Ed., "Liquid-Propellant Rocket Combustion Instability," NASA SP-194, Washington, D.C., Chaps. 3 and 4, 1972.

[6]Allison, C. B. and Faeth, G. M., "Open-Loop Response of a Burning Liquid Monopropellant," *AIAA Journal*, Vol. 13, Oct. 1975, pp. 1287-1294.

[7]Allison, C. B. and Faeth, G. M., "Decomposition and Hybrid Combustion of Hydrazine, MMH and UDMH as Droplets in a Combustion Gas Environment," *Combustion and Flame*, Vol. 19, Oct. 1972, pp. 213-226.

[8]Faeth, G. M., "Monopropellant Droplet Burning at Low Reynolds Numbers," *Combustion and Flame*, Vol. 11, April 1967, pp. 167-174.

[9]Faeth, G. M., "Flame Zone Development of Monopropellant Droplets," *Combustion and Flame*, Vol. 12, Oct. 1968, pp. 411-416.

[10]Faeth, G. M., "Prediction of Pure Monopropellant Droplet Life Histories," *AIAA Journal*, Vol. 8, July 1970, pp. 1308-1314.

[11]Chanin, S. P. and Faeth, G. M., "Oscillatory Combustion of Liquid Monopropellant Droplets," NASA CR-134983, Washington, D.C., 1976.

[12]Williams, F. A., *Combustion Theory*, Addison-Wesley, Reading, Mass, 1965, pp. 252.